Supporting Information

Blended Hole Transport Layer for Efficient and Stable Full-Color NiO_x-based QLEDs

Meng-Wei Wang, Yin-Man Song, Hang Liu, Ting Ding, Jing Jiang, Pei-Li Gao, Kar Wei Ng* and Shuang-Peng Wang**

Institute of Applied Physics and Materials Engineering, University of Macau, Taipa, Macao SAR 999078, China

* Corresponding author:

Pei-Li Gao (peiligao@um.edu.mo),

Kar Wei Ng (billyng@um.edu.mo),

Shuang-Peng Wang (spwang@um.edu.mo).

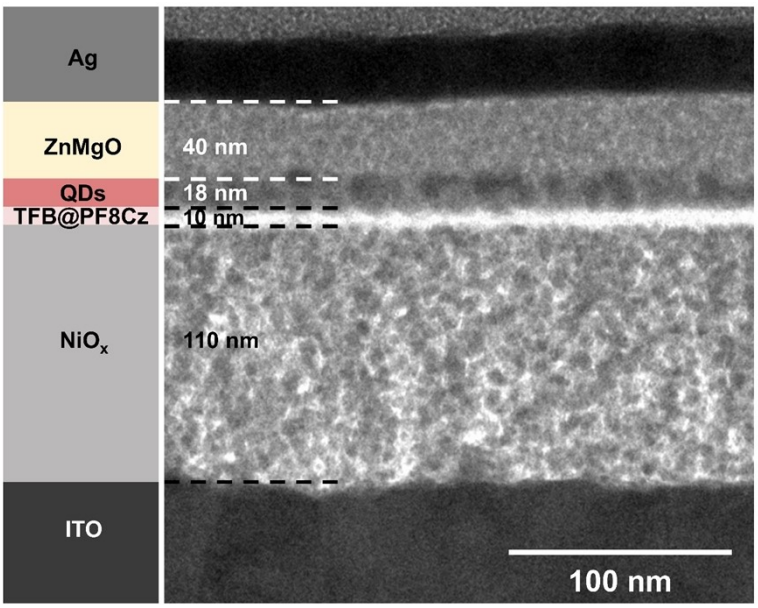

Fig. S1 Cross-sectional transmission electron microscope (TEM) image of the QLED device.

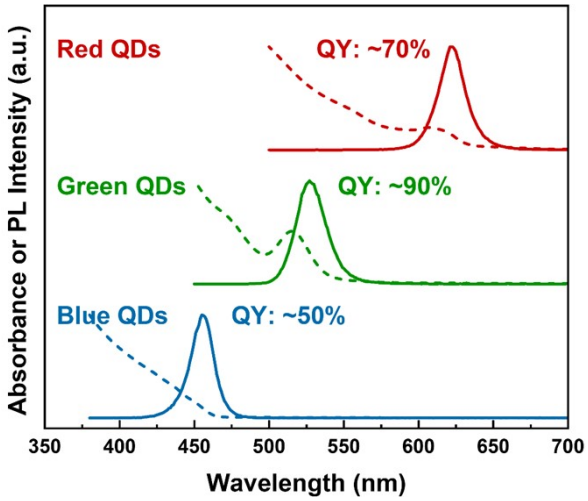

Fig. S2 Absorption spectra (dashed lines) and PL spectra (solid lines) of QDs solutions. The red, green, and blue QDs employed in this work are based on CdSe/ZnS core-shell structures. The emission peaks for the red, green, and blue QDs are centered at 620 nm, 525 nm, and 457 nm, respectively, with corresponding PLQYs of ~70%, ~90%, and ~50%. The absorption edges of the red, green, and blue QDs span 600-650 nm, 500-550 nm, and 425-475 nm, respectively, consistent with their bandgap-dependent optical properties.

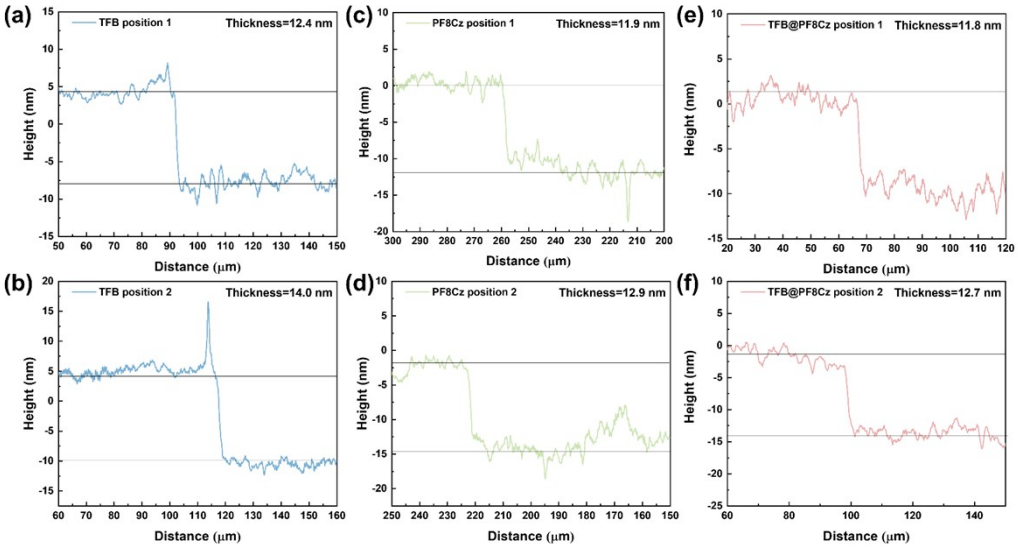

Fig. S3 Thickness of HTLs detected by film thickness tester. Thickness of (a) and (b) TFB film, (c) and (d) PF8Cz film, and (e) and (f) TFB@PF8Cz film.

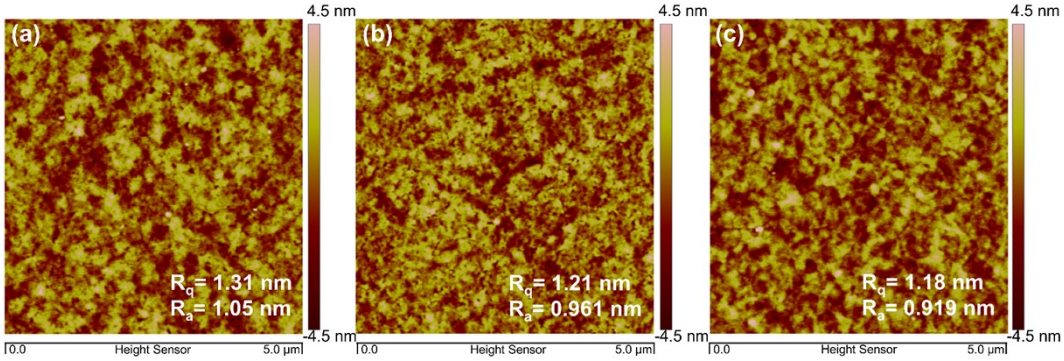

Fig. S4 Surface roughness of HTLs. AFM images of (a) TFB, (b) PF8Cz, and (c) TFB@PF8Cz films.

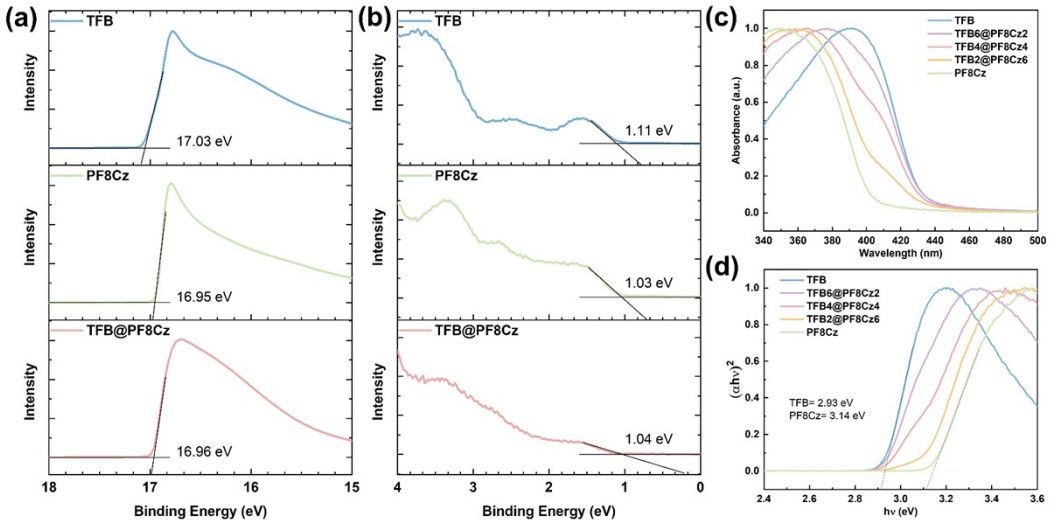

Fig. S5 Optical properties of materials. UPS spectra of TFB, PF8Cz, and TFB@PF8Cz films (a) in the cutoff and (b) in the onset regions. (c) UV-Vis absorption spectra and (d) Tauc´s plot for band gap determination of blended HTL with different PF8Cz ratios. According to the secondary electron cutoff edge of UPS spectra, the HOMO levels of TFB, PF8Cz and TFB@PF8Cz are all determined to be -5.3 eV. The optical band gaps of TFB and PF8Cz are 2.93 eV and 3.14 eV, respectively. The LUMO levels of TFB and PF8Cz are -2.37 eV and -2.16 eV, respectively. For the TFB@PF8Cz HTL, its LUMO level is between -2.37 eV and -2.16 eV, which is consistent with the tunable absorption band edge observed at different component ratios.

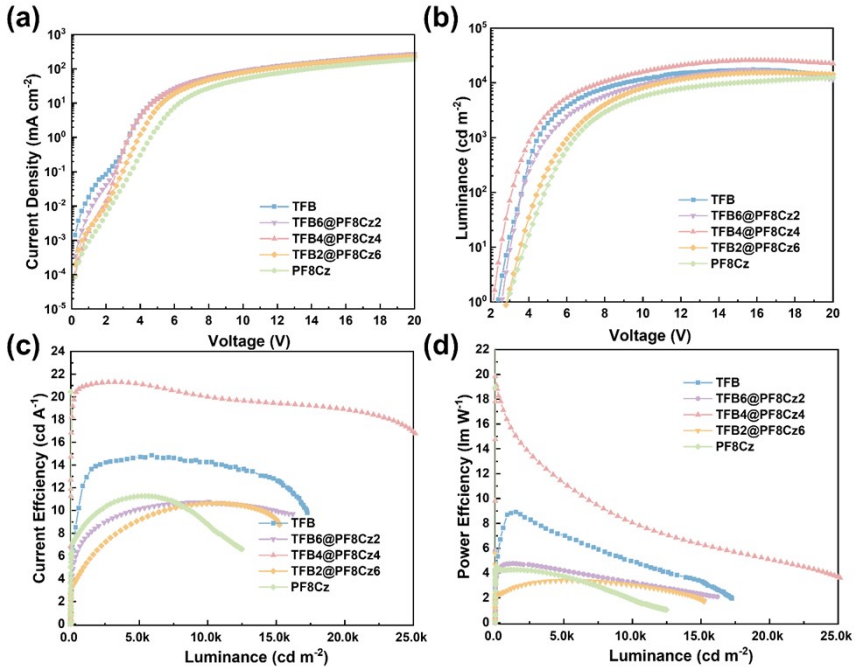

Fig. S6 Performance of NiO_x-based QLEDs with different HTLs. (a)J-V, (b) L-V, (c) CE-L, and (d) PE-L curves of QLEDs with different HTLs.

We fabricated QLEDs using five distinct HTL ratios: pure TFB, TFB6@PF8Cz2, TFB4@PF8Cz4, TFB2@PF8Cz6, and pure PF8Cz. Among these, the TFB QLED exhibited the highest current density, attributable to TFB's high hole mobility, whereas the PF8Cz QLED showed the lowest current density owing to PF8Cz's inferior hole mobility. As the PF8Cz ratio increased from 0 to 2 mg mL^{-1}, a significant reduction in leakage current was observed, likely due to electron blocking by PF8Cz's shallow LUMO level. This decrease in leakage current continued as the PF8Cz ratio rose to 4 and 6 mg mL^{-1}. Conversely, an increase in TFB ratio from 0 to 8 mg mL^{-1} led to a gradual rise in injection current. In the TFB4@PF8Cz4 QLED, an optimal balance between TFB's enhanced hole transport and PF8Cz's electron leakage blocking was achieved, resulting in superior performance.

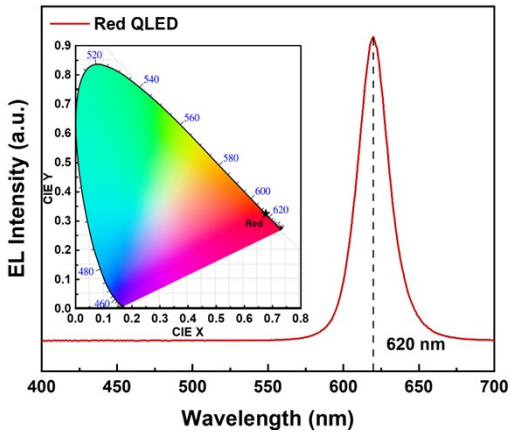

Fig. S7 The EL spectrum and CIE schematic diagram of the red QLED. The CIE coordinates are X=0.68, Y=0.33.

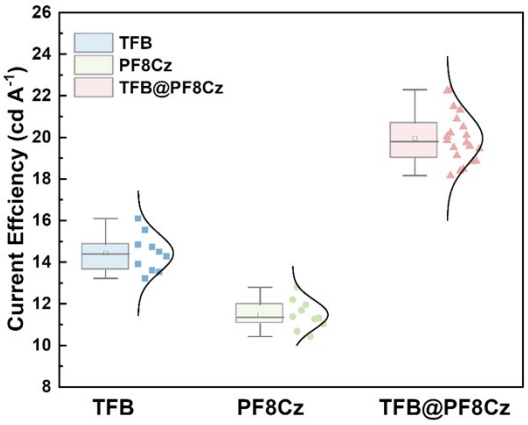

Fig. S8 The statistics of device peak CEs.

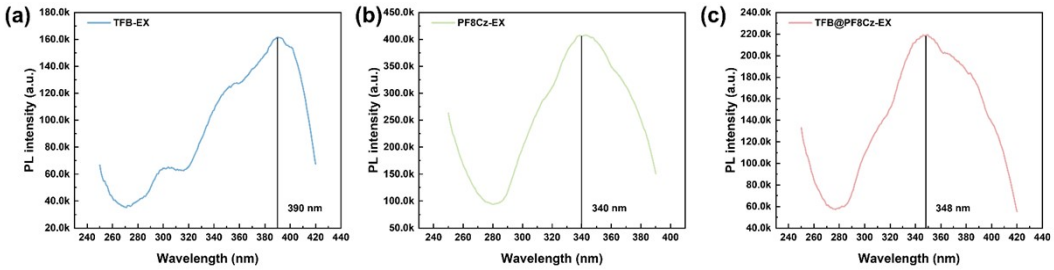

Fig. S9 PL excitation spectra of (a) TFB, (b) PF8Cz, and (c) TFB@PF8Cz films.

The optimal excitation wavelengths of TFB, PF8Cz, and TFB@PF8Cz films are 390 nm, 340 nm, and 348 nm, respectively.

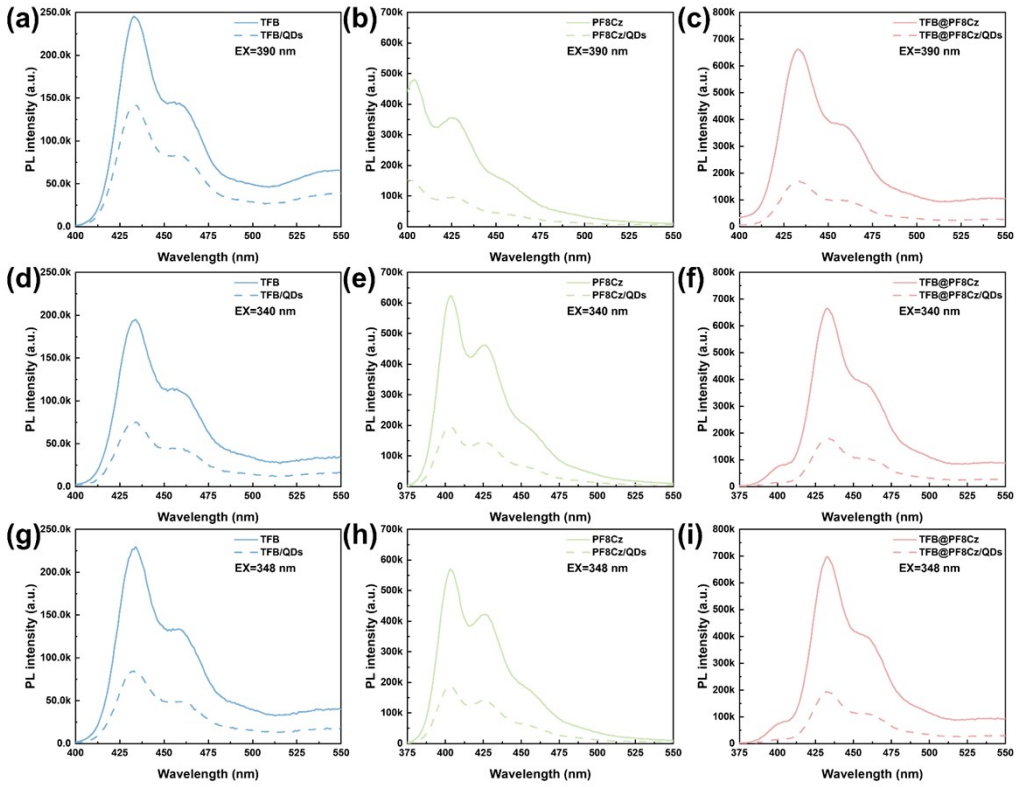

Fig. S10 (a)~(c) PL spectra of HTL and HTL/QDs films at the excitation wavelength of TFB at 390 nm. (d)~(f) PL spectra of HTL and HTL/QDs films at the excitation wavelength of PF8Cz at 340 nm. (g)~(i) PL spectra of HTL and HTL/QDs films at the excitation wavelength of TFB@PF8Cz at 348 nm.

The PL emission spectra of the three HTLs were measured at their corresponding excitation wavelengths. Results indicated that TFB@PF8Cz HTL consistently exhibited the highest PLQE, suggesting enhanced hole transfer.

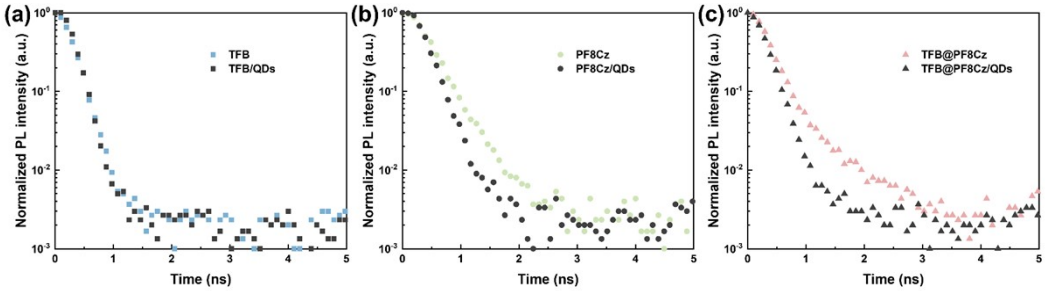

Fig. S11 TrPL spectra of (a) TFB, (b) PF8Cz, and (c) TFB@PF8Cz films before and after the deposition of the QDs layer.

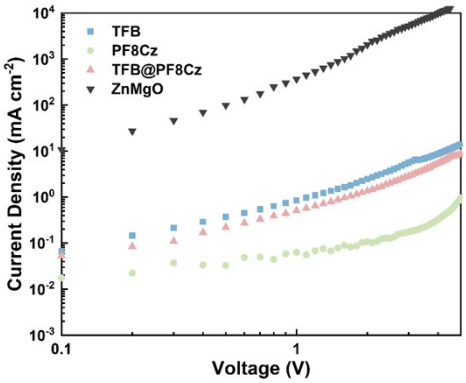

Fig. S12 J-V curves of hole-only device (ITO/NiO_x/HTLs/QDs/TCTA/MoO_3/Ag) and electron-only device (ITO/ZnMgO/QDs/ZnMgO/Ag).

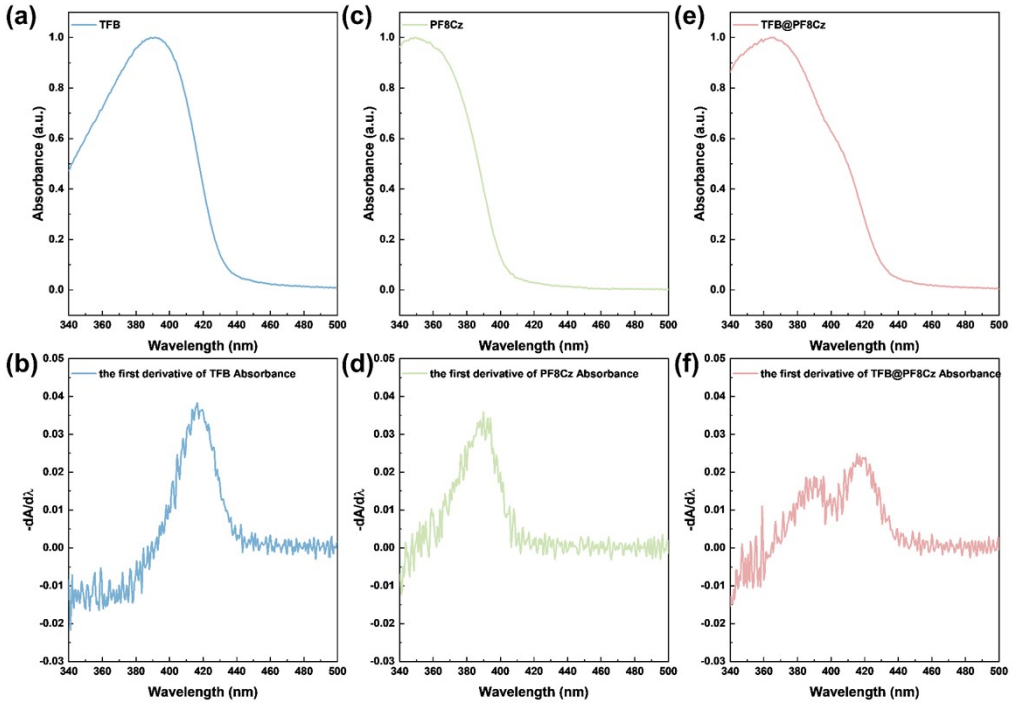

Fig. S13 Absorption spectra and the first derivative of absorption spectra. (a) and (b) are TFB film. (c) and (d) are PF8Cz film. (e) and (f) are TFB@PF8Cz film.

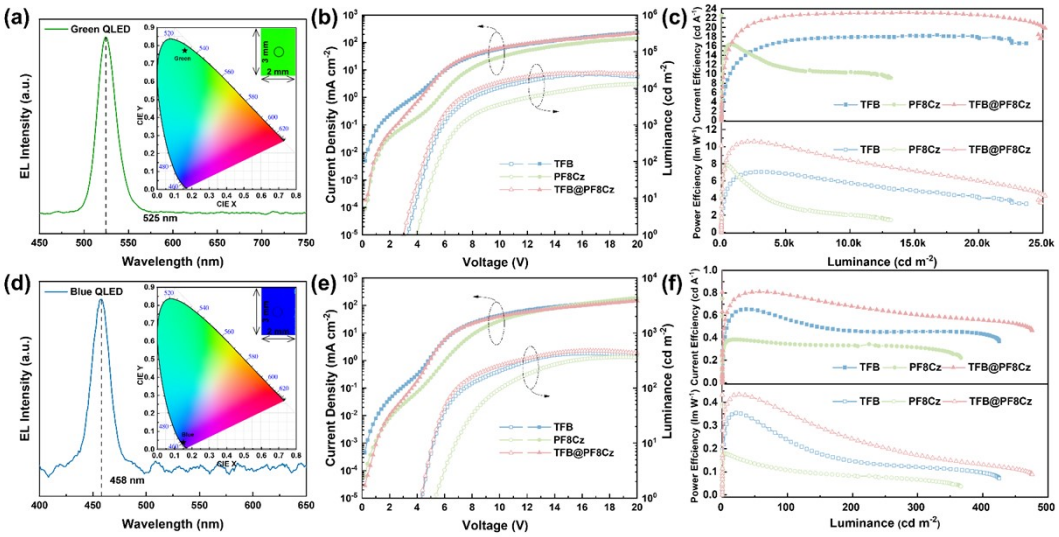

Fig. S14 Performance of green and blue NiO_x-based QLEDs with different HTLs. (a) EL spectra and CIE schematic diagram of green NiO_x-based QLEDs. The CIE coordinates are X=0.16, Y=0.77. (b) J-L-V curves and (c) CE-L and PE-L curves of green NiO_x-based QLEDs with three different HTLs. (d) EL spectra and CIE schematic diagram of blue NiO_x-based QLEDs. The CIE coordinates are X=0.15, Y=0.04. (e) J-L-V curves and (f) CE-L and PE-L curves of blue NiO_x-based QLEDs with three different HTLs.

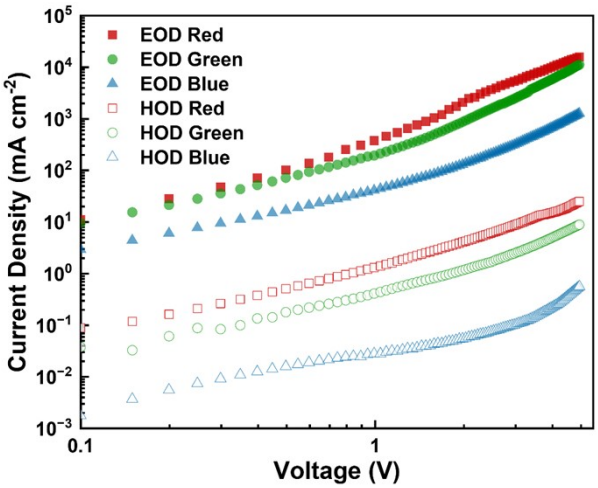

Fig. S15 The J-V characteristics of hole-only devices and electron-only devices. The device structure of HOD is ITO/NiO_x/TFB/QDs/TCTA/MoO_3/Ag. The device structure of EOD is ITO/ZnMgO/QDs/ZnMgO/Ag.

Table S1. PLQE values of three different HTLs at specific excitation wavelength.

λ	TFB	PF8Cz	TFB@PF8Cz
340 nm	0.595	0.680	0.726
348 nm	0.619	0.666	0.723
390 nm	0.418	0.710	0.744

Table S2. Device performances of QLEDs with different HTLs.

Devices	Peak EL (nm)	HTL	V_T (V)	Peak CE (cd A^{-1})	Peak L (cd m^{-2})	Peak PE (lm W^{-1})	Peak EQE (%)
Red	620	TFB	2.39	14.85	17253	8.93	8.96
		PF8Cz	2.89	11.27	12486	4.49	6.80
		TFB@PF8Cz	2.14	21.31	25769	19.14	12.86
Green	525	TFB	3.29	18.37	24694	7.05	4.69
		PF8Cz	3.96	16.37	13164	7.86	4.18
		TFB@PF8Cz	3.00	23.17	26447	10.61	5.92
Blue	458	TFB	4.36	0.66	425	0.35	1.81
		PF8Cz	5.33	0.38	366	0.18	1.04
		TFB@PF8Cz	4.27	0.81	476	0.43	2.22

EQE is calculated as follows:[1]

$$EQE = \frac{1.18 * \text{ current efficiency } * \pi * \text{ Emission wavelength}}{\text{Visual constant } * 10000}$$

1 S. R. Forrest, D. D. C. Bradley and M. E. Thompson, Adv. Mater., 2003, 15, 1043-1048.